

Resonant multiphoton ionization of H_2 via the $E, F \ ^1\Sigma_g^+$ state: Absorption of photons in the ionization continuum

C. Cornaggia, D. Normand, J. Morellec, G. Mainfray, and C. Manus

*Service de Physique des Atomes et des Surfaces, Commissariat à l'Energie Atomique,
Centre d'Etudes Nucléaires de Saclay, 91191 Gif-sur-Yvette Cédex, France*

(Received 7 January 1986)

This work reports the five-photon ionization of the H_2 molecule via the four-photon transitions ($E, F \ ^1\Sigma_g^+$, $v_E=1,2,3$) ← ($X \ ^1\Sigma_g^+$, $v=0$), in the 10^{11} -W/cm² laser-intensity range. The resulting H^+ - and H_2^+ -ion spectra exhibit essentially the $Q(J)$ resonances, and the ratio $[H^+]/[H_2^+]$ is found to increase drastically with the vibrational quantum number v_E . The photoelectron energy spectra are dominated by the peak corresponding to the five-photon ionization of H_2 leading to H_2^+ ions in the $v_+=v_E$ vibrational level. The photodissociation of H_2^+ is found to be the only process which forms H^+ . In addition, we report—for the first time, to our knowledge—the absorption by a molecule of an extra photon above the ionization potential, when the laser intensity is increased up to 7×10^{11} W/cm².

I. INTRODUCTION

Resonant multiphoton processes in H_2 have been recently investigated through photoion and photoelectron spectroscopy as well as through fluorescence measurements.¹⁻³ The ionization from various electronically excited states populated by multiphoton absorption has thus been studied, but in none of these experiments was the dissociation channel reported to play an important role.

In a recent publication⁴ on the five-photon ionization of H_2 with four-photon resonance on the $E, F \ ^1\Sigma_g^+$, $v_E=2$ level, we have reported the existence of significant H^+ production at laser intensities around 10^{11} W/cm². This phenomenon was not expected because the two main mechanisms capable of producing H^+ ions are supposed to have a low probability.

The first one is the dissociation of excited H_2 followed by the ionization of atomic fragments. However, because of the similarity of the potential curves of the resonant electronic state E and the $X \ ^2\Sigma_g^+$ ground state of H_2^+ , the $(4+1)$ photon process is expected to ionize the H_2 molecule rather than to dissociate it.

The second one is the photodissociation of the H_2^+ ions. However, in this experiment the vibrational levels of H_2^+ accessible with the energy of five photons are $v_+=0,1,2$ and have very low photodissociation cross sections in the 3850-Å spectral range.⁵ In particular, the photodissociation cross section of $v_+=2$ is predicted to be 1.3×10^{-23} cm² at 3850 Å. If we assume that the vibrational level $v_+=2$ was preferentially populated according to the Franck-Condon principle, a photodissociation of only a few percent is expected, which is 1 order of magnitude less than our observations.

Most likely, this discrepancy must be assigned to the influence of the laser field on the molecular potential: either the photodissociation cross section of H_2^+ , $v_+=2$ is enhanced under the high field conditions, or higher v_+ levels are populated, or the dissociation of H_2 is no longer negligible.

In order to understand the mechanism of the H^+ formation we have extended the investigation of the resonances to different vibrational levels ($v_E=0,1,2,3$) and measured the corresponding electron energy spectra. The results on the ion and electron spectra will be presented in Secs. III and IV, respectively, after a brief description of our experimental setup given in Sec. II. Finally, we report in Sec. V evidence for the absorption of an additional photon above the ionization potential of the H_2 molecule when the laser intensity is increased up to 7×10^{11} W/cm².

The study of the four-photon resonance on the first vibrational level ($v_E=0$) requires smaller photon energies.

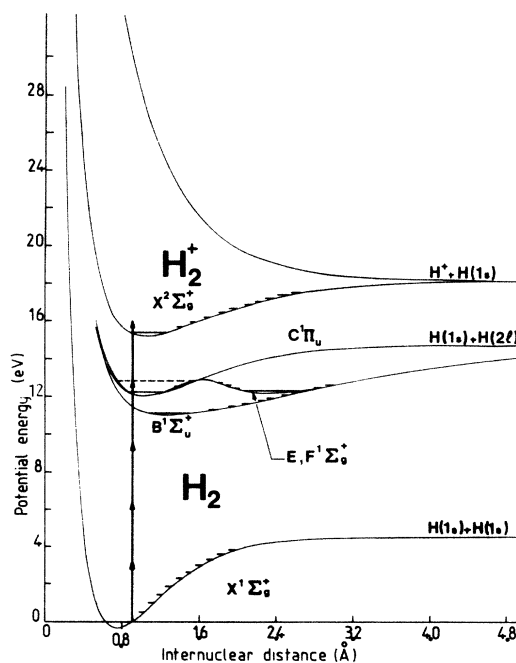


FIG. 1. Schematic energy diagram of H_2 .

This makes the ionization of H_2 a sixth-order process whereas it is only a fifth-order process for the resonances on the other v_E 's. For sake of clarity, the results concerning $v_E=0$ will therefore be presented separately.⁶ The schematic energy diagram of H_2 is shown in Fig. 1.

II. EXPERIMENTAL SETUP

A. Laser

The ionization of H_2 via the four-photon resonances ($E, F^1\Sigma_g^+, v_E=1,2,3 \leftarrow X^1\Sigma_g^+, v=0$) requires a high-power laser tunable in the (3800–4000)-Å spectral range. For this purpose we use a ruby-laser-pumped Jobin-Yvon dye laser which can deliver up to 250 mJ in 10 ns around 780 nm and up to 65 mJ after frequency doubling in a potassium dihydrogen phosphate (KDP) crystal. The laser wavelength is measured with a 1.15-m-long spectrometer to an accuracy of 0.08 Å. The laser linewidth is smaller than 0.5 cm^{-1} .

The laser beam is successively focused in two different cells (Fig. 2). The former is designed to allow a total collection of the photoions; the latter is equipped with an electron spectrometer to measure the energy distribution of the photoelectrons.

To permit an easy comparison of the ion and electron measurements, identical spherical lenses (focal length 150 mm) are used to focus the laser in both cells. The intensity distribution in the focal plane of the lens is recorded after enlargement on a silicium vidicon camera interfaced with an image digitizer.⁷ The beam cross section is measured to be $(6.5 \pm 0.8) \times 10^{-6} \text{ cm}^2$ at the best focus.

B. Ion detection

In the first cell, the photoions are created between two large parallel plates and drawn out of the interaction region by a uniform electric field of 270 V cm^{-1} . The ions are then time-of-flight (TOF) mass separated through a field-free space of 15 cm. The H^+ and H_2^+ signals are found to vary linearly with the H_2 pressure in the 10^{-5} – 10^{-3} Torr range. Our operating pressure is at most 5×10^{-4} Torr so that collective or collisional effects are

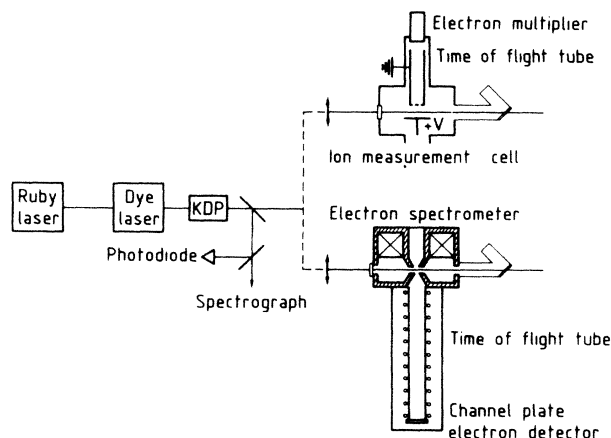


FIG. 2. Experimental apparatus.

negligible. The hydrogen gas we used is from l'Air Liquide, type N60, purity 99.9999%. Due to the use of a turbopump-diffusion pump system the residual pressure in the vacuum cell is as low as 10^{-8} Torr.

C. Electron spectrometer

In the second cell, the photoelectrons are analyzed with an electron spectrometer developed in the Fundamenteel Onderzoek der Materie (FOM) Institute for Atomic and Molecular Physics,⁸ and the measurements are performed under identical purity and pressure conditions for electrons and ions.

This spectrometer is a magnetic field parallelizer, with a magnetic field that diverges from 1 T at the laser focus to 10^{-3} T in the flight tube. The electrons originally emitted over 2π sr are formed into a parallel beam over a short distance so that the TOF is largely independent of the initial emission direction.

When the TOF is made as long as about $1 \mu\text{s}$ (by applying retarding voltages on the flight tube) the energy resolution can be as low as 20 meV. The electron spectrometer is calibrated by performing the multiphoton ionization of Xe atoms at 3884 Å. This yields electrons of 0.65 and 2.55 eV corresponding to the $^2P_{3/2}$ and $^2P_{1/2}$ continua, respectively. The calibration accuracy is within 0.1 eV.

III. ION RESULTS

A. General considerations

The vibrational quantum numbers $v_E=1,2,3$ correspond to Dieke's labels⁹ and are, respectively, $v=3,6,9$ in the full double-well potential curve.^{10,11} Whereas the $v_E=1$ and 2 levels are inside the E inner well, the $v_E=3$ level lies above the potential barrier and this could make the notation inadequate. However, for the sake of simplicity the v_E notation will be used throughout this paper.

In the resonant multiphoton ionization (RMPI) processes under investigation, the rotational selection rules for the four-photon transition $E, F^1\Sigma_g^+ \leftarrow X^1\Sigma_g^+$ are $\Delta J=0, \pm 2, \pm 4$, so that the Q, S, O, U, M branches are, in principle, observable. In fact, only the Q lines corresponding to the first four rotational levels of the $X^1\Sigma_g^+, v=0$ ground state have been detected in our experiment.

The one-photon coupling of the v_E resonant level with the ionization continuum is much stronger than the four-photon coupling of that resonant level with the ground state. Such a case is called a "crossing resonance."^{12,13} Ignoring the problems of the statistics of the laser light and the space-time distribution of the intensity, the RMPI probability, in the vicinity of the $Q(J)$ resonance, can be expressed as^{13,14}

$$W \cong \frac{I^5}{(\Delta_J - \alpha_J I)^2 + (\gamma_J I)^2}, \quad (1)$$

where Δ_J is the detuning from resonance, $\Delta_J = 4E_p - E(Q(J))$; α_J is the ac Stark shift of the $Q(J)$ transition; $\gamma_J I$ is the ionization rate of the resonant level ($E, F^1\Sigma_g^+, v_E, J$); I is the laser intensity; and E_p is the

photon energy.

Because of the laser-induced level shift and broadening, the probability W is no longer proportional to the fifth power of the laser intensity. The order of nonlinearity, $k = \partial \ln W / \partial \ln I$, is now a function of the photon energy and of the intensity. From Eq. (1) it can be easily shown that k takes a maximum value k_+ and a minimum value k_- which depend only on the ratio p between the broadening and the shift of the resonant level:

$$k_{\pm} = 5 \pm \frac{1}{p[(p^2 + 1)^{1/2} \pm p]} \quad \text{with } p = \gamma_J / \alpha_J. \quad (2)$$

Two typical situations may be encountered. (i) The shift of the resonant level is much larger than its broadening ($p \ll 1$); then Eq. (2) becomes

$$k_{\pm} \approx 5 \pm 1/p, \quad (3)$$

which shows that k undergoes very large variations.¹⁵ (ii) The broadening is equal to or larger than the shift ($p \gtrsim 1$); then Eq. (2) becomes

$$k_+ = 5 + 1/2p^2,$$

$$k_- = 3 + 1/8p^2.$$

In that case the variations of k are roughly within the interval 3–5, the value of 3 being reached on resonance.

Finally, it must be pointed out that the above considerations are only valid in the case of an isolated resonance. In most molecules, the situation is more complicated due to the presence of other quasis resonances which may contribute significantly to the total ion signals. In the present experiment, the variations of k are presented for $v_E = 1$ and 2 and tentatively interpreted. For $v_E = 3$ the RMPI cross section is weaker and the amplitude of our measurements is reduced, preventing a reliable determination of k .

B. $v_E = 1$

In the study of RMPI—especially for high-order processes—small fluctuations of the laser beam cross section of the laser pulse duration or phase fluctuations between modes can induce very large variations of the ion signals, even though the laser energy is kept perfectly constant. Therefore our experimental technique is to keep the laser wavelength λ constant and measure the ion signals N_i as a function of I . A least-squares fit of the data points—in ln-ln coordinates—then allows us to average the laser fluctuations and to determine accurately $N_i = f(I)$ for each λ . The slope of such a curve is the effective order of nonlinearity, $k_{\text{eff}} = \partial \ln N_i / \partial \ln I$, which is an approximate value of k in the laser-intensity range imposed by the RMPI process.

As an illustration, Fig. 3 represents the variations of the H₂⁺-ion signal in the case of the four-photon resonance on the $v_E = 1$ level. Curves *a* and *b* correspond, respectively, to $\lambda = 3943.16$ Å and $\lambda = 3945.67$ Å. The ion signal extends over 2 orders of magnitude, allowing an accurate determination of the slopes: k_{eff} is found equal to 2.8 ± 0.2 for curve *a* and to 5.8 ± 0.4 for curve *b*.

From a set of curves similar to those of Fig. 3, we can deduce the ion resonance profiles at a constant laser inten-

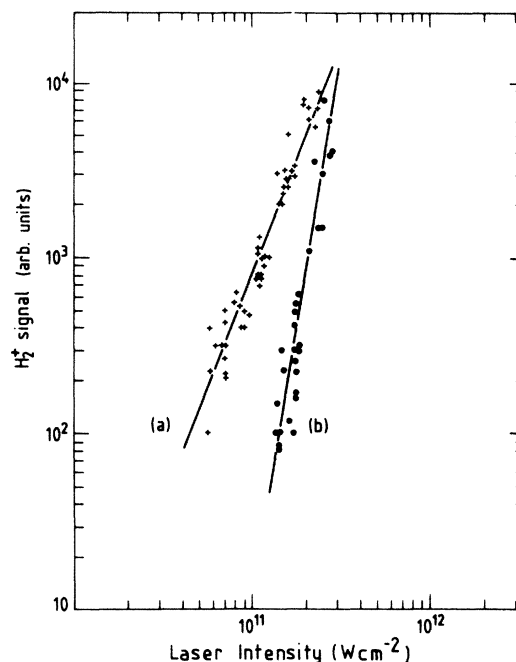


FIG. 3. Number of H₂⁺ ions as a function of the laser intensity for two different laser wavelengths: (a) $\lambda = 3943.16$ Å, (b) $\lambda = 3945.67$ Å.

sity (Fig. 4). Only H₂⁺ ions corresponding to the Q lines are detected here. The H⁺ signal is vanishingly small. Given our ion threshold detectivity, the ratio $[H^+]/[H_2^+]$ is estimated to be smaller than 1%.

The H₂⁺ spectra are presented at two different intensities: $I_1 = (0.9 \pm 0.2) \times 10^{11}$ W/cm² and $I_2 = (1.5 \pm 0.3) \times 10^{11}$ W/cm². The $Q(J)$ peaks ($J = 0, 1, 2, 3$) appear blue shifted from their zero-field positions as the laser intensity is increased. The $E, F^1\Sigma_g^+, v_E$ term values are obtained from the $E-B$ lines positions of Dieke⁹ and the $B-X$ measurements of Wilkinson.¹⁶ (They are equivalent to Dieke's tables of term values of $E, F^1\Sigma_g^+$ using the usual +8-cm⁻¹ correction.^{11,17}) A rough estimate of the $Q(1)$ peak displacement leads to a value of $10 \text{ cm}^{-1} / 10^{11} \text{ W cm}^{-2}$. As a comparison, in two-photon fluorescence studies, Pummer *et al.*¹⁸ obtained a similar value of the ac Stark shift, but with photon energies twice as big as ours.

Figure 5 represents the variations of k_{eff} as a function of the four-photon energy. The profile is essentially characterized by large asymmetric minima centered at the $Q(J)$ resonances where k_{eff} is found equal to 3. Unambiguously, this slope of 3 is not due to a saturation of the RMPI process. Indeed, even for the highest intensity (2.5×10^{11} W/cm²) on the strongest line, we estimate that only one molecule out of 1000 is ionized in the interaction volume. This corresponds to an ionization probability of 10^5 s^{-1} .

In addition, k_{eff} hardly exceeds the value of 5 which is the value expected off resonance. From the considerations of Sec. III A, we deduce that the ionization width of the resonant level (induced by the coupling with the continuum) must be of the order of the ac Stark shift. As an illustration we compare in Fig. 6 the values of k_{eff} mea-

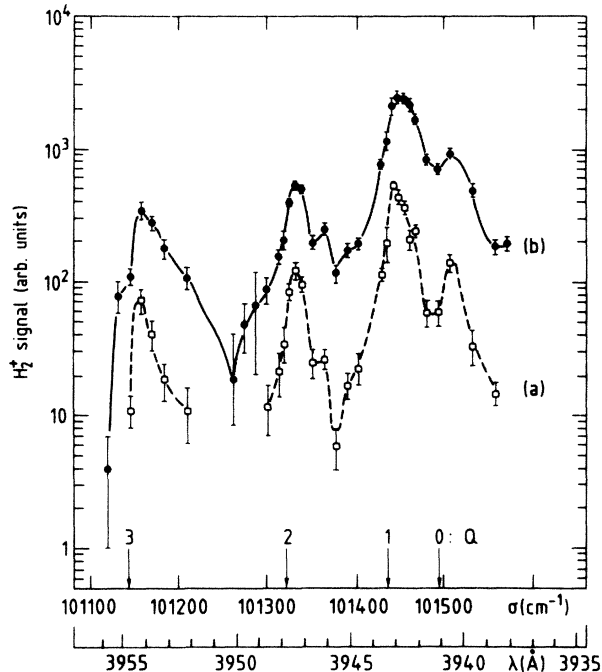


FIG. 4. Relative multiphoton ionization cross section for the production of H_2^+ via the Q four-photon transitions ($E, F^1\Sigma_g^+, v_E=1 \leftarrow (X^1\Sigma_g^+, v=0, J_X)$) for two laser intensities: (a) $(0.9 \pm 0.2) \times 10^{11} \text{ W cm}^{-2}$, (b) $(1.5 \pm 0.3) \times 10^{11} \text{ W cm}^{-2}$. σ is the energy of four photons (cm^{-1}) and λ is the laser wavelength (\AA). The four-photon laser bandwidth is smaller than 2 cm^{-1} .

sured in the vicinity of the strongest resonance [$Q(1)$] with three calculations corresponding, respectively, to $p=0.3, 1,$ and 2 . Our energy resolution, albeit poor, is enough to show that the curve $p=2$ is the best fit. The laser-induced broadening of the resonant level can then be estimated to be $40 \text{ cm}^{-1}/10^{11} \text{ W cm}^{-2}$, full width at half

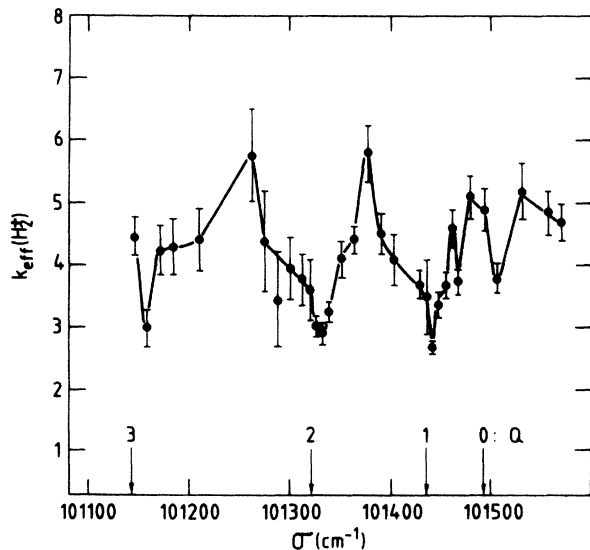


FIG. 5. Variations in $k_{\text{eff}} = \partial \ln N_i / \partial \ln I$ as a function of the energy of four photons in the conditions of Fig. 4.

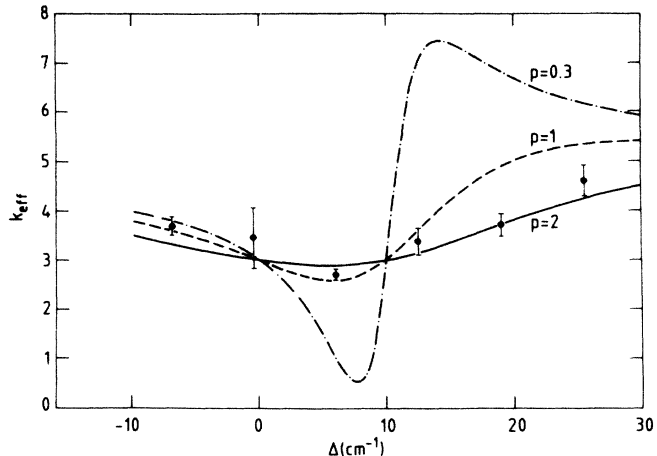


FIG. 6. Variations in the effective order of nonlinearity in the five-photon ionization of H_2 via the $Q(1)$ four-photon resonance ($E, F^1\Sigma_g^+, v_E=1 \leftarrow (X^1\Sigma_g^+, v=0)$) as a function of Δ . Δ is the static detuning $\Delta = 4\hbar\omega - E(Q(1))$. p is the ratio between the broadening and the shift of the resonant level. \bullet are experimental points.

maximum (FWHM). The photoionization cross section of the $v_E=1$ level is thus of the order of 10^{-17} cm^2 at 3943 \AA . Under a photon flux of 2×10^{29} photons/ $\text{cm}^2 \text{ s}$, the photoionization of the resonant level is completely saturated which confirms *a posteriori* the hypothesis of the crossing resonance.

To summarize, we have been able to carry out a semi-quantitative analysis of our data on the strongest resonance in the case of $v_E=1$. However, it is obvious that a more sophisticated model should be developed to take into account the space-time distributions of the laser light,¹⁹ the influence of the other $Q(J)$ resonances on the behavior of a particular $Q(J_0)$ resonance, and the contribution of possible five-photon resonances with Rydberg states above the ionization potential.

C. $v_E=2$

Figure 7 represents the number of H^+ and H_2^+ ions as a function of the laser wavelength for a laser intensity of $(1.5 \pm 0.3) \times 10^{11} \text{ W/cm}^2$. This result has been discussed elsewhere.⁴ The ratio $[H^+]/[H_2^+]$ is much larger than for the $v_E=1$ case. Its value is 20% when the resonance $Q(1)$ is achieved and exceeds 100% on the blue wing of the $Q(0)$ line. Both H^+ and H_2^+ spectra exhibit essentially the $Q(J)$ four-photon resonances, indicating that the dissociation process sets in at energies above the E, F state.

The inversion between H^+ and H_2^+ profiles around 103650 cm^{-1} has been found to be reproducible, but remains unexplained. It does not correspond to any resonance on the inner (E) nor the outer (F) potential wells. Furthermore, the electron spectra (Sec. IV) do not reveal any particular peak assignable to the two-photon ionization of H ($n=2$) which could have accounted for the previously suggested mechanism of five-photon resonant predissociation of the $3p\pi D^1\Pi_u^+, v=10$ by the $B^1\Sigma_u^+$

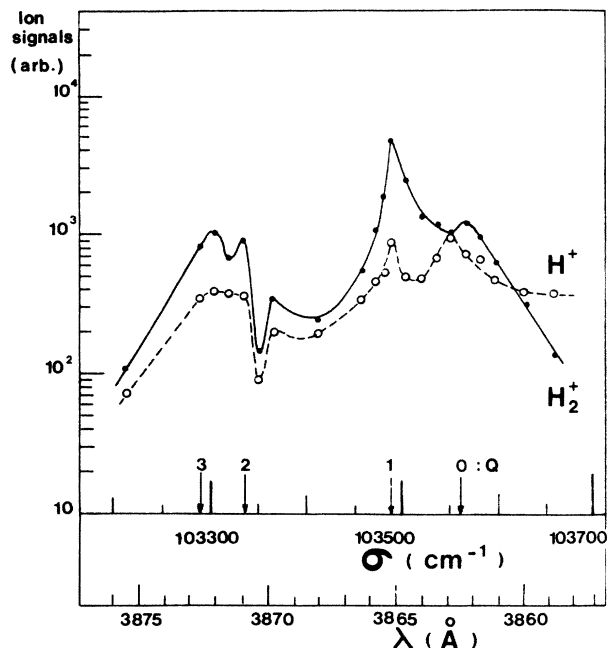


FIG. 7. Comparison of the H₂⁺- and H⁺-ion production in the multiphoton ionization of H₂ via the *Q* four-photon transitions ($E, F^1\Sigma_g^+, v_E=2$) ← ($X^1\Sigma_g^+, v=0, J_X$). The laser intensity is $(1.5 \pm 0.3) \times 10^{11}$ W cm⁻².

state. Further investigations are necessary to identify the enhancement of H⁺ in that energy range.

Figure 8 represents the variations in the effective order of nonlinearity k_{eff} as a function of the four-photon energy. For the sake of clarity, the k_{eff} profiles have been drawn separately for the H⁺- and H₂⁺-ion signals. The

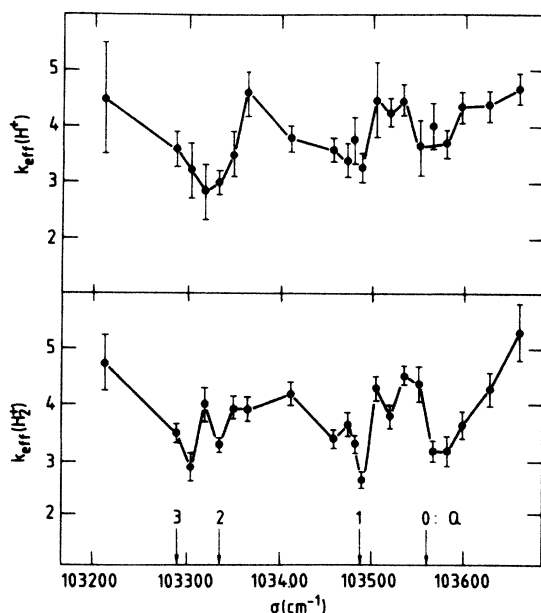


FIG. 8. Variations in $k_{\text{eff}} = \partial \ln N_i / \partial \ln I$ as a function of the energy of four photons in the conditions of Fig. 7, for H⁺ and H₂⁺.

main observation is that both profiles are quite similar, which proves that H⁺ and H₂⁺ signals are essentially governed by the four-photon transition from the $X^1\Sigma_g^+$ to the $E, F^1\Sigma_g^+$ states. This remark rules out the possibility that H⁺ is formed through direct absorption—from the $X^1\Sigma_g^+$ ground state—of more than five photons, in which case k_{eff} would be on the whole higher for H⁺ than for H₂⁺. As a consequence, we expect H⁺ to be formed through a stepwise process, the second step requiring the absorption of a small number of photons, so that the intensity dependence of the H⁺ signal is governed by the first step.

Similarly to our observation for $v_E=1$, the onset of each $Q(J)$ resonance is marked, on the k_{eff} profiles, by a minimum value close to 3. In addition, the k_{eff} values keep within the interval 3–5 in the whole spectral range investigated. As stated before, this indicates the predominance of the laser-induced level broadening over the ac Stark shift.

D. $v_E=3$

For the four-photon resonances on $v_E=3$, only the $Q(0)$ and $Q(1)$ lines have been investigated (Fig. 9). The RMPI probability is here lower than for $v_E=1$ and 2. Consequently, the laser intensity is increased to $(2.3 \pm 0.4) \times 10^{11}$ W/cm² to keep the ion yield in the same range.

The most obvious difference from the previous resonances investigated is that, for $v_E=3$, the H⁺ signal strongly dominates the H₂⁺ signal throughout the energy domain of 200 cm⁻¹. The ratio [H⁺]/[H₂⁺] is found equal to 3.5 and is almost independent of the photon energy. The width of the $Q(1)$ resonance peaks is about 25 cm⁻¹ (FWHM), which corresponds to a photoionization

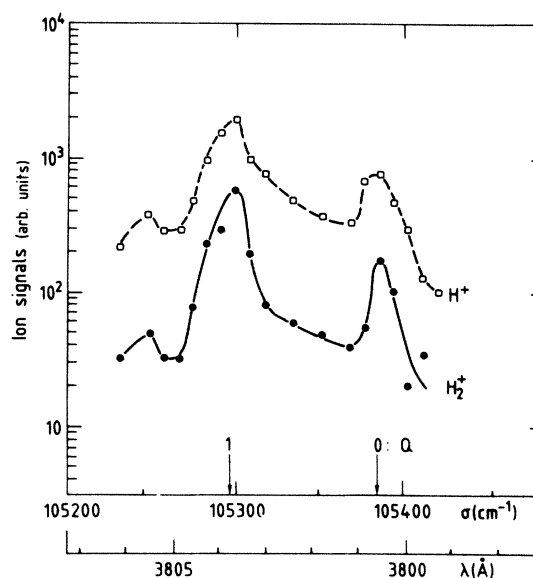


FIG. 9. Comparison of the H₂⁺- and H⁺-ion productions in the multiphoton ionization of H₂ via the *Q* four-photon transitions ($E, F^1\Sigma_g^+, v_E=3$) ← ($X^1\Sigma_g^+, v=0, J_X$). The laser intensity is $(2.3 \pm 0.4) \times 10^{11}$ W cm⁻².

cross section of $\nu_E=3$ of the order of $2 \times 10^{-18} \text{ cm}^2$.

When comparing the $\nu_E=1,2,3$ ion profiles, it appears that the enhancement of the ion yield at resonance is less and less pronounced as the photon energy is tuned through higher and higher vibrational levels of the E,F double well. Indeed, the range of variation of the $\text{H}^+ + \text{H}_2^+$ signal is about 2 orders of magnitude for $\nu_E=1$, but it hardly exceeds a factor 10 for $\nu_E=3$.

Finally, we performed a short experiment on $\nu_E=4$ to measure the ion spectrum in the very vicinity of the $Q(1)$ line. Only H^+ ions are detected. Given our threshold detectivity, the ratio $[\text{H}^+]/[\text{H}_2^+]$ is assumed to be larger than 100.

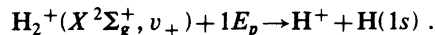
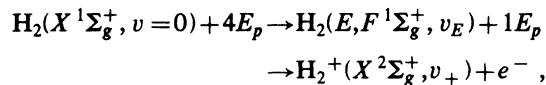
E. CONCLUSION

All the ion-spectra measurements presented in this section can be condensed into Fig. 10 where the ratio $[\text{H}^+]/[\text{H}_2^+]$ taken at the top of the $Q(1)$ line is plotted against the vibrational quantum number ν_E . The figure points out two essential conclusions.

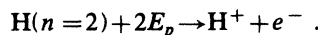
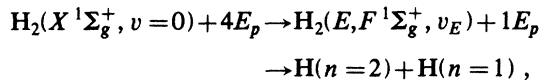
(i) The ratio $[\text{H}^+]/[\text{H}_2^+]$ increases by 4 orders of magnitude when tuning the resonance from $\nu_E=1$ to $\nu_E=4$.

(ii) Within the laser-intensity range imposed by the four-photon transition, the ratio $[\text{H}^+]/[\text{H}_2^+]$ is roughly independent of the laser intensity.

In addition, we have shown that the H^+ resonance spectra are mainly governed by the four-photon resonances $(E, F^1\Sigma_g^+, \nu_E) \leftarrow (X^1\Sigma_g^+, \nu=0)$. From these considerations, two stepwise processes A and B are likely to contribute to the H^+ formation. Process A is



Process B is



Process A is the photodissociation of H_2^+ while process B is the dissociation of the neutral molecule via excited (pre)dissociative states followed by the two-photon ionization of $\text{H}(n=2)$ atoms. The electrons arising from processes A and B are, respectively, released by the H_2 molecule and the $\text{H}(n=2)$ atoms. Therefore, photoelectron spectroscopy is the most convenient way to estimate the respective contribution of A and B to the H^+ formation.

IV. PHOTOELECTRON SPECTRA IN THE $10^{11} \text{ W cm}^{-2} - 3 \times 10^{11} \text{ W cm}^{-2}$ LASER-INTENSITY RANGE

We report in this section the electron spectra following the multiphoton ionization and dissociation of H_2 in the $10^{11} \text{ W cm}^{-2} - 3 \times 10^{11} \text{ W cm}^{-2}$ intensity range where the ion measurements have been performed. The laser wavelength is tuned to the $Q(1)$ four-photon resonance $(E, F^1\Sigma_g^+, \nu_E, J_E=1) \leftarrow (X^1\Sigma_g^+, \nu=0, J_X=1)$ for $\nu_E=1,2,3$. According to the foreseen processes A and B, two electron classes are expected.

(i) Slow electrons ($E < 0.5 \text{ eV}$) corresponding to final vibrational states ($\nu_+ \leq \nu_E$) of the H_2^+ ion for the five-photon ionization of H_2 (process A).

(ii) Fast electrons of energy around 3 eV arising from the two-photon ionization of $\text{H}(n=2)$ atoms (process B).

Figure 11 shows the electron-energy spectra measured for $\nu_E=1,2,3$ at a laser intensity $I = (3 \pm 0.6) \times 10^{11} \text{ W cm}^{-2}$. The main characteristic of these spectra is that all the electron peaks originate from the five-photon ionization of the H_2 molecule. There is no electron peak arising from the ionization of $\text{H}(n=2)$ atoms. Therefore, all the H^+ -ion spectra presented in Sec. III result from the five-photon ionization of the molecules followed by a partial photodissociation of the molecular ions (process A). Another important result is that the $\nu_+ = \nu_E$ final vibrational state of the H_2^+ ion is found to be the most populated as expected from the Franck-Condon principle.

The small influence of the laser intensity on the ion vibrational distribution is clear in Fig. 12 where the electron spectrum for $\nu_E=1$ is obtained at a lower laser intensity $I = 1.2 \times 10^{11} \text{ W cm}^{-2}$. The width of the peaks is found to be equal to 40 meV. Taking the ratio of the peak areas gives the branching ratio of the ν_+ populations: 92% for $\nu_+=1$ and 8% for $\nu_+=0$.

An estimate of the photodissociation cross sections of H_2^+ for $\nu_+=1,2,3$ is now possible assuming that to a good approximation the final vibrational state of H_2^+ is exclusively $\nu_+ = \nu_E$. These experimental values are compared with Dunn's photodissociation cross sections⁵ in

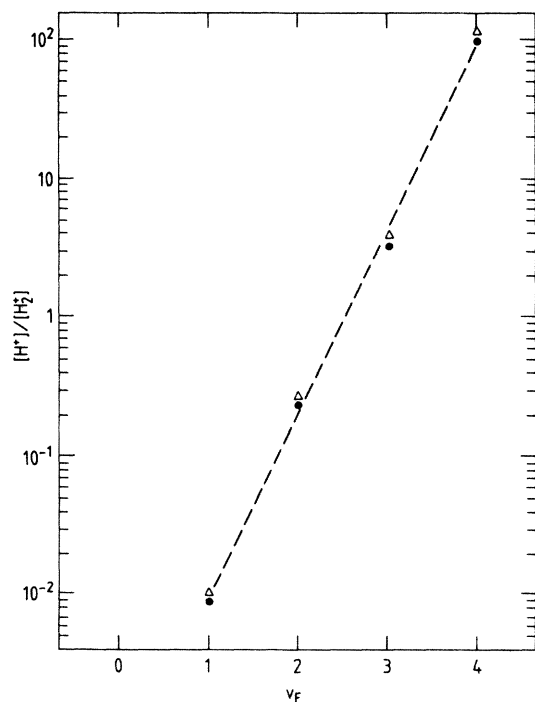


FIG. 10. Variation of the $[\text{H}^+]/[\text{H}_2^+]$ ratio as a function of the four-photon resonant vibrational state ν_E at the top of the $Q(1)$ line. ●, $I = (1.5 \pm 0.3) \times 10^{11} \text{ W cm}^{-2}$. △, $I = (2.0 \pm 0.4) \times 10^{11} \text{ W cm}^{-2}$.

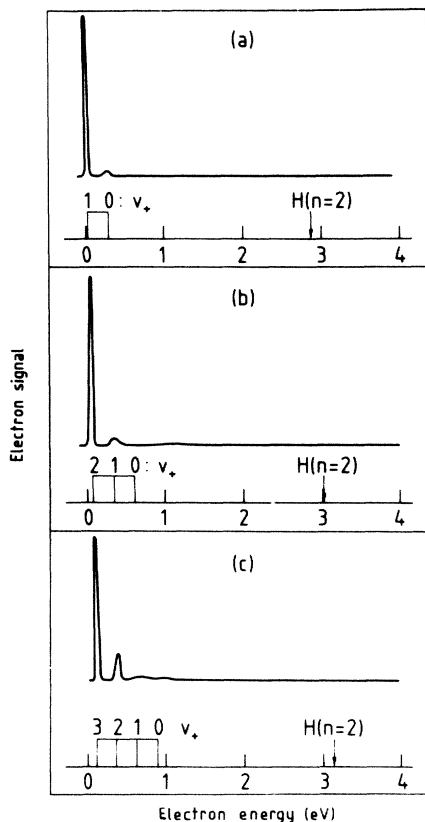


FIG. 11. Photoelectron spectra following the five-photon ionization of H₂ via the $Q(1)$ four-photon transition ($E, F^1\Sigma_g^+, v_E=1, 2, 3$) $\leftarrow (X^1\Sigma_g^+, v=0)$. (a) $v_E=1$, (b) $v_E=2$, (c) $v_E=3$. The laser intensity is $(3.0 \pm 0.6) \times 10^{11} \text{ W cm}^{-2}$. v_+ ($\leq v_E$) are the expected final vibrational states of the H₂⁺ ion. The arrow "H ($n=2$)" indicates the energy of electrons expected from the two-photon ionization of H ($n=2$) atoms.

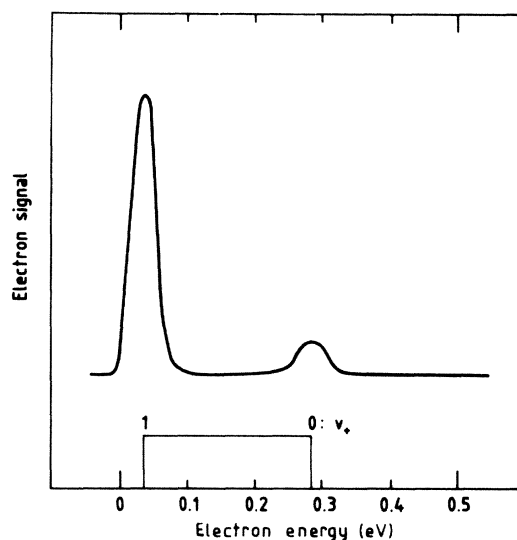


FIG. 12. Photoelectron spectrum following the five-photon ionization via the $Q(1)$ four-photon transition ($E, F^1\Sigma_g^+, v_E=1$) $\leftarrow (X^1\Sigma_g^+, v=0)$. The laser intensity is $(1.2 \pm 0.2) \times 10^{11} \text{ W cm}^{-2}$.

TABLE I. Comparison of the calculated (Ref. 5) and measured photodissociation cross sections of the vibrational levels $v_+=1, 2, 3$ of H₂⁺, $X^2\Sigma_g^+$. λ is the laser wavelength corresponding to the four-photon transition ($E, F^1\Sigma_g^+, v_E = v_+, J=1$) $\leftarrow (X^1\Sigma_g^+, v=0, J=1)$.

v_+	λ (Å)	σ (cm ²) (this experiment)	σ (cm ²) (theory)
1	3943	$< 5 \times 10^{-24}$	4×10^{-27} ^a
2	3865	10^{-22}	1.2×10^{-23}
3	3804	10^{-21}	6.6×10^{-21}

^aIn Ref. 5 the table giving the photodissociation cross section of $v_E=1$ ends at $\lambda=3500$ Å and yields the value of $5 \times 10^{-25} \text{ cm}^2$. A crude extrapolation up to $\lambda=3943$ Å leads to $4 \times 10^{-27} \text{ cm}^2$.

Table I at the laser wavelengths which correspond to the four-photon transition ($E, F^1\Sigma_g^+, v_E=1, 2, 3$) $\leftarrow (X^1\Sigma_g^+, v=0)$. The variation of the photodissociation cross sections as a function of v_+ is found to be significantly smaller than expected. This discrepancy is not explained but could result from the influence of the high laser field on the ground and dissociative electronic states of H₂⁺. In addition, it is possible that the two-photon dissociation of the $X^2\Sigma_g^+, v_+$ vibrational levels into the $X^2\Sigma_g^+$ dissociation continuum is no longer negligible at high intensity. The contribution of such a process could be particularly significant for $v_+=1$ and 2 since their photodissociation probability (one-photon process) is very weak.

V. PHOTOELECTRON SPECTRA IN THE 10^{12} W/cm^2 LASER-INTENSITY RANGE: ABOVE THRESHOLD IONIZATION

The absorption of photons above the ionization threshold in atoms is now a current subject of both experimental and theoretical studies.²⁰ Such processes are referred to as above threshold ionization (ATI) or "continuum-continuum" transitions. To our knowledge they have never been demonstrated in molecules through photoelectron spectroscopy. However, in large molecules they have been sometimes considered in order to explain the various mechanisms of fragmentation.²¹ In addition, Miller and Compton²² reported an electron peak in NO corresponding to the absorption of four photons when only three photons were required to exceed the ionization potential. However, in their experiment the three-photon ionization through the two-photon resonance on the $A^2\Sigma^+, v=3$ state is Franck-Condon forbidden as indicated by the authors. On the other hand, in the present experiment (Fig. 13) the five-photon ionization via the $E, F^1\Sigma_g^+, v_E$ four-photon resonant step is Franck-Condon permitted.

Figure 14 represents the electron spectra recorded at the laser intensity $I=(7 \pm 1.4) \times 10^{11} \text{ W cm}^{-2}$. The laser wavelength is tuned to the $Q(1)$ four-photon resonance ($E, F^1\Sigma_g^+, v_E, J_E=1$) $\leftarrow (X^1\Sigma_g^+, v=0, J_X=1)$ with $v_E=1, 2, 3$. The labels ($v_+ 5E_p$) and ($v_+ 6E_p$) correspond to the absorption of five and six photons by the H₂ molecule

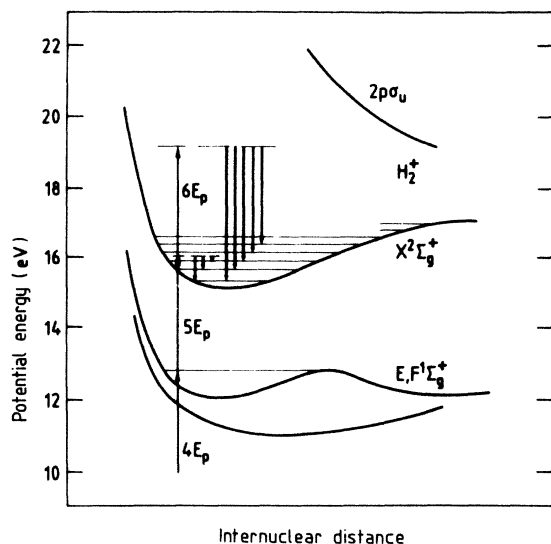
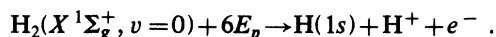


FIG. 13. Schematic energy-level diagram relevant to the photoelectron spectra when one additional photon is absorbed above the ionization potential.

in its ground state. The slow-electron peaks (five-photon ionization) have roughly the same characteristics as in the lower intensity range $10^{11} \text{ W cm}^{-2} - 3 \times 10^{11} \text{ W cm}^{-2}$: the $v_+ = v_E$ electron peak dominates the other peaks as expected from the Franck-Condon principle. The broad electron peak around 1 eV remains unexplained. Nevertheless, a process which is energetically possible but Franck-Condon forbidden may be a direct dissociative ionization from the $X^1\Sigma_g^+, v=0$ ground state:



The absorption of one more photon above the ionization potential leads to several final vibrational states of the H_2^+ ion close to $v_+ = v_E$. Thus the vibrational distribution of the H_2^+ ions remains strongly affected by the four-photon resonant vibrational state v_E . However, the $v_+ = v_E$ peak no longer dominates the other peaks: possible five-photon quasiresonances with Rydberg states of H_2 may affect the final vibrational distribution of the H_2^+ ions originating from the six-photon ionization of H_2 .

VI. CONCLUSION

The five-photon ionization of H_2 via the four-photon resonances $(E, F^1\Sigma_g^+, v_E = 1, 2, 3) \leftarrow (X^1\Sigma_g^+, v=0)$ has been investigated in the $10^{11} - 10^{12} \text{ W cm}^{-2}$ laser-intensity range through photoion and photoelectron spectroscopy. The resulting H^+ and H_2^+ spectra exhibit essentially the four-photon $Q(J)$ resonances, the ratio $[\text{H}^+]/[\text{H}_2^+]$ increasing drastically with v_E .

In the $10^{11} \text{ W cm}^{-2} - 3 \times 10^{11} \text{ W cm}^{-2}$ range, the electron energy spectra show only two peaks: one peak contains about 90% of the photoelectrons and is associated with $\text{H}_2^+, v_+ = v_E$; the other one is associated with $\text{H}_2^+, v_+ = v_E - 1$. There is no evidence of peaks arising from the ionization of excited H atoms. The dissociation

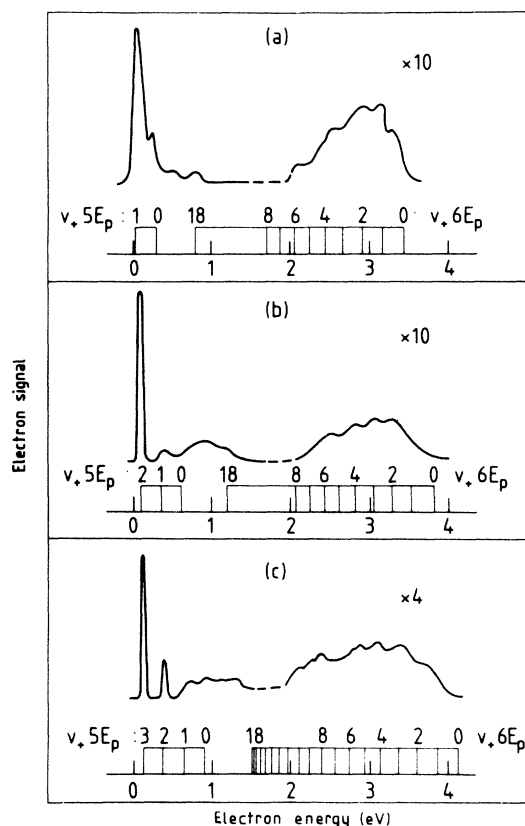


FIG. 14. Photoelectron spectra following the five- and six-photon (one additional photon above the ionization potential) ionization of H_2 via the $Q(1)$ four-photon transition $(E, F^1\Sigma_g^+, v_E) \leftarrow (X^1\Sigma_g^+, v=0)$. (a) $v_E=1$, (b) $v_E=2$, (c) $v_E=3$. The laser intensity is $(7.0 \pm 1.4) \times 10^{11} \text{ W cm}^{-2}$.

of the neutral molecule by the laser light is found negligible.

Consequently, the observed H^+ signals can only originate from the photodissociation of the H_2^+ ions. Our measured photodissociation cross sections of H_2^+, v_+ increase very rapidly with the vibrational number v_+ . Yet this increase is not so steep as theoretically predicted, the high laser field probably being responsible for the discrepancy.

At higher laser intensity ($7 \times 10^{11} \text{ W cm}^{-2}$) we demonstrate the absorption by the neutral molecule of an additional photon above the ionization potential $X^2\Sigma_g^+$. Although the absorption of the six photons brings the molecule above 18 eV, the H_2^+ population remains distributed over vibrational levels close to $v_+ = v_E$. Contrary to the five-photon process, the six-photon process does not follow the Franck-Condon principle, since a large number of vibrational levels are populated, with equivalent populations.

ACKNOWLEDGMENTS

The authors are grateful to R. Boudigues, M. Bougeard, D. Fondant, C. Robine, and A. Sanchez for their skilled technical assistance.

- ¹D. J. Kligler and C. K. Rhodes, *Phys. Rev. Lett.* **40**, 309 (1978); D. J. Kligler, J. Bokor, and C. K. Rhodes, *Phys. Rev. A* **21**, 607 (1980).
- ²S. L. Anderson, G. D. Kubiak, and R. N. Zare, *Chem. Phys. Lett.* **105**, 22 (1984).
- ³S. T. Pratt, P. M. Dehmer, and J. L. Dehmer, *J. Chem. Phys.* **78**, 4315 (1983); *Chem. Phys. Lett.* **105**, 28 (1984).
- ⁴C. Cornaggia, J. Morellec, and D. Normand, *J. Phys. B* **18**, L501 (1985).
- ⁵G. H. Dunn, *Phys. Rev.* **172**, 1 (1968); Joint Institute for Laboratory Astrophysics Report No. 92, 1968 (unpublished).
- ⁶D. Normand, C. Cornaggia, and J. Morellec (unpublished).
- ⁷L. A. Lompré, G. Mainfray, and J. Thébault, *Rev. Phys. Appl.* **17**, 21 (1982).
- ⁸P. Kruit and F. H. Read, *J. Phys. E* **16**, 313 (1983).
- ⁹G. H. Dieke, *Phys. Rev.* **50**, 797 (1936).
- ¹⁰W. Kolos and L. Wolniewicz, *J. Chem. Phys.* **50**, 3228 (1969).
- ¹¹L. Wolniewicz and K. Dressler, *J. Mol. Spectrosc.* **67**, 416 (1977).
- ¹²C. Cohen-Tannoudji, *Cargese Lectures in Physics*, edited by M. Levy (Gordon and Breach, New York, 1967), Vol. 2, p. 347.
- ¹³Y. Gontier and M. Trahin, *Phys. Rev. A* **19**, 264 (1979).
- ¹⁴G. Petite, J. Morellec, and D. Normand, *J. Phys. (Paris)* **40**, 115 (1979).
- ¹⁵J. Morellec, D. Normand, and G. Petite, *Phys. Rev. A* **14**, 300 (1976).
- ¹⁶P. Wilkinson, *Can. J. Phys.* **46**, 1225 (1968).
- ¹⁷G. Herzberg and L. L. Howe, *Can. J. Phys.* **37**, 636 (1959).
- ¹⁸H. Pummer, H. Egger, T. S. Luk, T. Srinivasan, and C. K. Rhodes, *Phys. Rev. A* **28**, 795 (1983).
- ¹⁹M. Poirier, J. Reif, D. Normand, and J. Morellec, *J. Phys. B* **17**, 4135 (1984).
- ²⁰P. Agostini, F. Fabre, G. Mainfray, G. Petite, and N. K. Rahman, *Phys. Rev. Lett.* **42**, 1127 (1979); P. Kruit, J. Kimman, H. G. Muller, and M. J. van der Wiel, *Phys. Rev. A* **28**, 248 (1983); Y. Gontier, M. Poirier, and M. Trahin, *J. Phys. B* **13**, 1381 (1981); J. Kupersztych (unpublished).
- ²¹T. E. Carney and T. Baer, *J. Chem. Phys.* **75**, 4422 (1981), and references therein.
- ²²J. C. Miller and R. N. Compton, *J. Chem. Phys.* **75**, 22 (1981).